7688–7701 Nucleic Acids Research, 2011, Vol. 39, No. 17 Published online 7 June 2011
doi:10.1093/nar/gkr406

Roles of Trm9- and ALKBH8-like proteins in the formation of modified wobble uridines in *Arabidopsis* tRNA

Vibeke Leihne[1], Finn Kirpekar[2], Cathrine B. Vågbø[3], Erwin van den Born[1], Hans E. Krokan[3], Paul E. Grini[1], Trine J. Meza[1] and Pål Ø. Falnes[1,*]

[1]Department of Molecular Biosciences, University of Oslo, P.O. Box 1041 Blindern, 0316 Oslo, Norway, [2]Department of Biochemistry and Molecular Biology, University of Southern Denmark, 5230 Odense M, Denmark and [3]Department of Cancer Research and Molecular Medicine, Norwegian University of Science and Technology, 7489 Trondheim, Norway

Received April 8, 2011; Revised April 29, 2011; Accepted May 2, 2011

ABSTRACT

Uridine at the wobble position of tRNA is usually modified, and modification is required for accurate and efficient protein translation. In eukaryotes, wobble uridines are modified into 5-methoxycarbonylmethyluridine (mcm^5U), 5-carbamoylmethyluridine (ncm^5U) or derivatives thereof. Here, we demonstrate, both by *in vitro* and *in vivo* studies, that the *Arabidopsis thaliana* methyltransferase AT1G31600, denoted by us AtTRM9, is responsible for the final step in mcm^5U formation, thus representing a functional homologue of the *Saccharomyces cerevisiae* Trm9 protein. We also show that the enzymatic activity of AtTRM9 depends on either one of two closely related proteins, AtTRM112a and AtTRM112b. Moreover, we demonstrate that AT1G36310, denoted AtALKBH8, is required for hydroxylation of mcm^5U to (*S*)-$mchm^5U$ in $tRNA^{Gly}_{UCC}$, and has a function similar to the mammalian dioxygenase ALKBH8. Interestingly, *atalkbh8* mutant plants displayed strongly increased levels of mcm^5U, and also of mcm^5Um, its 2′-*O*-ribose methylated derivative. This suggests that accumulated mcm^5U is prone to further ribose methylation by a non-specialized mechanism, and may challenge the notion that the existence of mcm^5U- and mcm^5Um-containing forms of the selenocysteine-specific $tRNA^{Sec}$ in mammals reflects an important regulatory process. The present study reveals a role in for several hitherto uncharacterized *Arabidopsis* proteins in the formation of modified wobble uridines.

INTRODUCTION

tRNA molecules typically contain several different post-transcriptional modifications, and such modifications are essential for tRNA function. Located at specific sites throughout the tRNA body they facilitate correct folding and contribute to stabilizing the tertiary structure (1,2). Moreover, modifications on the anticodon stem–loop (ASL) are important to ensure efficient and accurate decoding during translation, as well as to maintain a correct reading frame (3–5).

The nucleoside at the wobble position (position 34), which base pairs with the nucleoside in the third position of the codon, is frequently modified. In particular, a uridine at this position (U34) almost invariably carries a modification. Cytoplasmic tRNAs in eukaryotes usually harbour the U34 modifications 5-methoxycarbonylmethyluridine (mcm^5U), 5-carbamoylmethyluridine (ncm^5U) or derivatives thereof (6). The biogenesis of these modifications have been studied in most detail in *Saccharomyces cerevisiae*. Here, the Elongator complex, consisting of the six proteins Elp1–6, is required for the early steps in the synthesis of modified wobble uridines and, interestingly, the phenotypes of Elongator mutants are suppressed by over-expression of certain tRNAs that are hypomodified in these mutants (7,8). The formation of mcm^5U from 5-carboxymethyluridine (cm^5U) is catalysed by the methyltransferase Trm9 (9). Several mcm^5U-containing tRNAs are further modified by thiolation, a modification that

*To whom correspondence should be addressed. Tel: +47 91151935; Fax: +47 22854443; Email: pal.falnes@imbv.uio.no

The authors wish it to be known that, in their opinion, the last two authors should be regarded as joint Last Authors.

restricts wobbling, yielding 5-methoxycarbonylmethyl-2-thiouridine (mcm^5s^2U) (10). Accordingly, these thiolated tRNAs decode in the split codon boxes, where purine- and pyrimidine ending codons encode different amino acids. In contrast, ncm^5U-containing tRNAs generally decode in the 'family' codon boxes, where all four codons encode the same amino acid.

Several additional wobble uridine modifications not found in *S. cerevisiae* are present in mammals. The selenocysteine specific tRNA ($tRNA^{Sec}$) exists as two differentially modified subpopulations; one containing mcm^5U at the wobble position and another, which contains its 2′-*O*-ribose methylated derivative 5-methoxycarbonylmethyl-2′-*O*-methyluridine (mcm^5Um) in this position (11). In addition, two diastereomers of hydroxylated mcm^5U, (*R*)-$mchm^5U$ and (*S*)-$mchm^5U$ are found in mammalian $tRNA^{Arg}_{UCG}$ and $tRNA^{Gly}_{UCC}$, respectively (12).

Mammals have nine homologues, ALKBH1-ALKBH9, of the *Escherichia coli* dioxygenase AlkB, a DNA repair protein that uses an oxidative mechanism to remove deleterious methyl groups from DNA (13–18). Mammalian ALKBH8 consists of three domains, i.e. an N-terminal RNA recognition motif (RRM), followed by the characteristic AlkB-like dioxygenase domain, and a C-terminal methyltransferase (MT) domain. The MT domain of ALKBH8 was recently shown to represent the mammalian homologue of *S. cerevisiae* Trm9, and to be required for mcm^5U formation in mice (19,20). Similar to yeast Trm9, the MT domain of ALKBH8 forms a heterodimeric complex with TRM112, and this interaction is required for MT activity. In two recent studies, the RRM/AlkB moiety of mammalian ALKBH8 was demonstrated to catalyse the hydroxylation of mcm^5U into (*S*)-$mchm^5U$ in $tRNA^{Gly}_{UCC}$ (12,21).

In plants, the knowledge about tRNA modifications and their formation is limited, and only a handful studies have focused on tRNA modifying enzymes. The yeast Mod5 protein is an isopentenyltransferase responsible for generating isopentenyladenosine (i^6A) at position 37, and the corresponding *Arabidopsis* homologue has been identified and functionally characterized (22). Additionally, an *Arabidopsis* orthologue of the mammalian methyltransferases Dnmt2, which generates 5-methylcytosine in tRNA, has been identified (23). Recently, the modifications ncm^5U and mcm^5s^2U were reported to be present in *Arabidopsis* total tRNA, and their formation was shown to depend on a functional Elongator complex (24). Finally, a reverse genetics approach recently identified five tRNA modification genes in *Arabidopsis* (25).

In the present study, we have identified and characterized two novel tRNA modification enzymes in *Arabidopsis*, denoted AtTRM9 and AtALKBH8. While AtTRM9 displays similarity to the yeast Trm9 protein, AtALKBH8 shows similarity to the RRM/AlkB part of mammalian ALKBH8. Using AtTRM9 and AtALKBH8 loss-of-function mutants, as well as *in vitro* enzymatic assays, we demonstrate that AtTRM9 is a methyltransferase required for mcm^5U formation, while AtALKBH8 is the hydroxylase generating (*S*)-$mchm^5U$ from mcm^5U. Finally, we show that the MT-activity of AtTRM9 is dependent on either of the two *Arabidopsis* TRM112 homologues, AtTRM112a and AtTRM112b.

MATERIALS AND METHODS

Protein sequence analysis

Multiple sequence alignments were generated using MAFFT algorithm (26) embedded in the JalView alignment editor (27).

Plant materials

All plant lines were obtained from the Nottingham Arabidopsis Stock Centre (NASC) unless otherwise stated. Wild-type (WT) *Arabidopsis* (*Arabidopsis thaliana* ecotype Col-0) were grown in perlite soil at 18°C under 16 h of light at 100 $\mu E/m^2/s$. For axenic growth, seeds were surface sterilized in 7.5% hypochlorite solution containing 0.1% Tween-20, followed by treatment with 70% EtOH and washing in distilled water. Sterilized seeds were plated on solidified MS medium (28), supplemented with 2% sucrose (MS-2), kept in the dark at 4°C for 2 days and then transferred to 18°C.

For genotyping of T-DNA insertional mutants, genomic DNA was isolated from true leaves using the Ultraprep Plant DNA kit (AHN Biotechnologie). Homozygous *atalkbh8-1* plants were screened by PCR using a T-DNA right border primer 1 (RB1) and genomic primer G1, as well as a T-DNA left border primer 1 (LB1) combined with genomic primer G2 (See Supplementary Table S1 for details on DNA primers used in the present work). For screening of *atalkbh8-2* plants, the genomic primers G3 and G4 were used in combination with the LB primer. For *attrm9* plants, the PCR was conducted using the primer LB2 in combination with genomic primers G5 and G6. PCR products were cloned into the TOPO Blunt vector (Invitrogen), and sequenced to verify the integration site.

To analyse the expression of *AtALKBH8* and *AtTRM9* in the T-DNA lines, RNA was first isolated from liquid N_2 frozen tissue utilizing MagNA Lyser Green Beads (Roche Diagnostics), and subsequently purified using Spectrum Plant Total RNA Kit (Fluka/Sigma-Aldrich) followed by cDNA synthesis using Superscript II Reverse Transcriptase (Invitrogen) and a poly dT primer (Invitrogen). The expression of different regions upstream or downstream of the T-DNA insertion sites in the homozygous mutant lines was analysed as follows: for *AtALKBH8*, primers Up8-f/Up8-r were utilized to analyze expression upstream of the T-DNA integration site; primers Dwn8-f/Dwn8-r to examine expression downstream of the T-DNA insertion and primers Sp8-f/Sp8-r are spanning the T-DNA insertion. For *AtTRM9*, the following primers were utilized: primers Dwn9-f/Dwn9-r for investigating expression downstream of the T-DNA insertion and primers Sp9-r/Sp9-f that span the T-DNA insertion.

For scoring of seed germination in the different mutant plant lines, seeds were incubated in Petri dishes containing MS-2 medium supplemented with 1% (w/v) agar, for 48 h at 4°C, and then moved to a growth chamber at 22°C. All mutants were compared with WT from the same harvest.

Testa rupture was scored every day using a LEICA EZ4 microscope (New York Microscope Company Inc, New York, USA). For assessing root growth, seeds were processed as above. Plates were placed vertically and the number of lateral roots were determined over a 8-day period using a LEICA EZ4 microscope.

For tRNA isolation, seeds from homozygous mutant and WT plants were surface sterilized and plated on MS2. Two weeks after germination, the seedlings were frozen in liquid N_2 before grinding and isolation of tRNA.

Plasmid construction

The coding sequences of *AtTRM9* and *AtALKB8* were amplified by PCR from *Arabidopsis* cDNA templates using primer sets AtTRM9-f/AtTRM9-r and AtALKBH8-f/AtALKBH8-r, respectively, and subsequently cloned between the NdeI and BamHI restriction sites in the expression vector pET28a to generate pET28-AtTRM9 and pET28-AtALKB8. The coding sequence of AtTRM112a was PCR amplified from cDNA clone RAFL22-14-D01 [RIKEN Bio Research Centre (http://www.brc.riken.go.jp/)] using primers AtTRM112a-r and AtTRM112a-f, whereas AtTRM112b was amplified from cDNA clone U22673 {ABRC [Arabidopsis Biological Research Centre (www.abrc.osu.edu)]} using primers AtTRM112b-r and AtTRM112b-f. The PCR products were subsequently cloned between the NdeI and BglII sites of the second MCS in pET-Duet1 (Novagen), yielding pDuet-AtTRM112a and pDuet-AtTRM112b, respectively. To obtain pDuet-AtTRM9/AtTRM112a and pDuet-AtTRM9/AtTRM112b, a XbaI–BamHI fragment from pET28 to AtTRM9 was transferred to the first MCS of either pDuet-AtTRM112a or pDuet-AtTRM112b, respectively.

Protein purification

All recombinant proteins were expressed and purified from *E. coli* BL21-CodonPlus(DE3)-RIPL (Stratagene). Bacteria were grown at 16°C in LB medium containing 0.075 mM IPTG. Cell pellets were resuspended in ice-cold equilibration buffer [50 mM sodium phosphate pH 7.6, 150 mM NaCl, 10% glycerol, 0.5% NP-40, protease inhibitors (complete EDTA-free protease inhibitor tablets, Roche) and 0.5 mg/ml lysozyme (Fluka/Sigma-Aldrich], and lysates were generated utilizing a French press (Thermo IEC). Proteins were subsequently purified from pre-cleared lysates using TALON Metal Affinity Resin (Clontech) according to the manufacturer's instructions.

Total tRNA and tRNA isoacceptor isolation from plants

Six-hundred milligram of seedlings were harvested and homogenized in liquid nitrogen. Lysates were prepared by adding 9 ml of ice-cold lysis buffer [4 M guanidine thiocyanate, 100 mM Tris–HCl, 25 mM $MgCl_2$, 2% Triton X-100 (v/v), 25 mM EDTA, pH 7.5] to the homogenized tissue, followed by the addition of 9 ml of 3 M NaOAc. Total RNA was precipitated from the lysates with isopropanol, and the tRNA fraction was subsequently isolated using a RNA/DNA maxi kit (Qiagen). $tRNA^{Gly}_{UCC}$ was isolated from *Arabidopsis* total tRNA by hybridization to an immobilized oligonucleotide (Supplementary Table S1) using a protocol described previously (20).

Liquid chromatography coupled to tandem mass spectrometry (LC-MS/MS) analysis

LC-MS/MS analysis of nucleosides was essentially done as described (20). In brief, tRNA was enzymatically digested to nucleosides, which were separated by reverse phase high performance liquid chromatography (HPLC) on a Zorbax SB-C18 column, using a mobile phase consisting of 0.1% formic acid and a gradient of 5–50% methanol. Online mass spectrometry detection was performed using an Applied Biosystems/MDS Sciex 5000 triple quadrupole mass spectrometer (Applied Biosystems Sciex) with TurboIonSpray probe operating in positive electrospray ionization mode. The nucleosides were monitored by multiple reaction monitoring (MRM) using the nucleoside to base ion mass transitions 317.2→185.1 (mcm^5U), 333.2→201.1 ($mchm^5U$), 303.2→171.1 (cm^5U), 333.2→201.1 (mcm^5s^2U), 302.2→170.1 (ncm^5U), 318.2→186.1 (ncm^5s^2U), 268.2→136.1 (A), 244.2→112.1 (C), 284.2→152.2 (G) and 245.2→113.1 (U). Quantitation was accomplished by comparison with pure nucleoside standards run intermediate the samples. In the case of mcm^5Um, no nucleoside standard was available, but our previous studies on mammalian $tRNA^{Sec}_{UCA}$ indicate that mcm^5U and mcm^5Um display similar responses in the mass spectrometer, and this was used to estimate the mcm^5Um levels.

RNase T1 digestion and MALDI-TOF mass spectrometry

RNase T1 digestion of nucleosides and MALDI-TOF mass spectrometry were done as described previously (20).

Saponification of *S. cerevisiae* tRNA

To remove the methyl moiety from the methoxycarbonylmethyl group, the methyl ester linkage was broken by saponification of the tRNA substrate as described previously (20). Briefly, 10 µl of a tRNA solution was mixed with 1.25 µl of 1 M NaOH and the mixture was incubated at room temperature for 8 min. The solution was neutralized by the addition of 1.25 µl of 1 M acetic acid.

In vitro enzyme assays

For the methyltransferase assay, 5 and 10 µg total tRNA from plant and yeast (Roche), respectively, was incubated with AtTRM9 in the absence or presence of co-expressed AtTRM112a/b for 12 min at 37°C in 50 µl reaction buffer containing 1 µl *S*-adenosyl-*l*-[*methyl*-^{3}H]methionine (GE Healthcare), 50 mM Tris–HCl pH 7.5, 25 mM KCl, 25 mM NH_4OAc, 0.5 mM $MgCl_2$, 0.5 mM EDTA, 1 U RNasin Plus RNase Inhibitor (Promega). The reaction was stopped by adding 10% ice-cold TCA followed by 30 min incubation on ice. The reaction mixture was carefully applied to glass microfiber filters (GE-Healthcare) mounted to a filter holder manifold (Millipore) under vacuum. Subsequently, the filters were washed with 10% TCA followed by 96% ethanol, dried and added to

scintillation vials for measuring incorporation of radiolabelled methyl groups.

In the assay for hydroxylation of mcm^5U in *atalkbh8* tRNA, 5 μg tRNA was incubated with different amounts of the N-terminal part (amino acids 1–354) of human ALKBH8 for 30 min at 37°C in a 50 μl reaction mixture containing 50 mM Tris–HCl pH 7.5, 0.5 mM $MgCl_2$, 2 mM ascorbic acid, 100 μM 2-oxoglutarate, 40 μM $FeSO_4$, 10 U RNase inhibitor and then precipitated with 1 volume of isopropanol in the presence of 1 M NH_4Ac and 20 μg of glycogen. Pellets were washed with 70% EtOH and dried, before they were further processed for LC–MS/MS analysis.

RESULTS

In silico identification of ALKBH8/Trm9-like proteins in plants

During our efforts to characterize the mammalian ALKBH8 protein, we became intrigued by the observation that the RRM/AlkB and MT functions of ALKBH8 appeared to be encoded by two separate genes in plants. A protein BLAST search using human ALKBH8 as query retrieved two major hits in *Arabidopsis*, encoded by the genes *At1g31600* and *At1g36310*. The protein encoded by *At1g31600* displays high similarity to the N-terminal part of ALKBH8, encompassing the RRM and AlkB domains, and will be referred to as AtALKBH8. The protein encoded by *At1g36310* is highly similar to the C-terminal MT domain of human ALKBH8, as well as to the *S. cerevisiae* Trm9 protein, and was denoted AtTRM9. Putative orthologues of these two ALKBH8/Trm9-like proteins were found in other plants, such as rice (*Oryza sativa*) and grape (*Vitis vinifera*), showing that the separation of the dioxygenase and MT functions of ALKBH8 into two proteins, as observed in *Arabidopsis*, applies to both monocots and eudicots, and therefore might apply to land plants in general. Alignments of AtALKBH8 and AtTRM9 with putative orthologues from various organisms are shown in Figure 1A and B, respectively.

Annotation data, as well as available ESTs and cDNAs, suggest that alternative splicing may give rise to two different forms of the AtALKBH8 protein (Figure 2A and B). A 7 exon gene model (At1g31600.1) encodes a 431 amino acids protein (AtALKBH8a), whereas the alternative 8 exon model (At1g31600.2) encodes a 344 amino acids protein (AtALKBH8b) (Figure 2B). AtALKBH8a represents an extension of AtALKBH8b by 83 amino acids, but this extension shares no detectable sequence homology with any other proteins in the NCBI protein sequence database. Putative ALKBH8 orthologues from other plants lack a corresponding extension, and they are generally very similar in size to the 344 amino acids AtALKBH8b protein, to which they align throughout their entire sequence. Interestingly, the 159 nt DNA sequence encoding the N-terminal part (53 amino acids) of the 83 amino acid extension is highly similar (94% sequence identity) to the Ac-type transposon Tag2. This transposon, and inactive remnants thereof, are found in numerous copies throughout the *Arabidopsis* genome, indicating that the alternative splice form may have arisen through a transposition event (29). RT–PCR experiments showed that mRNAs corresponding to both forms of *AtALKBH8* were expressed in all tissues examined (stamen, rosette leaves, flowers and silique) (Figure 2C).

Two different gene models for the *At1g36310* gene have been predicted, consisting of two or three exons. The transcripts resulting from these gene models only differ in their 5′-UTR, and both encode the same 404 amino acid AtTRM9 protein. Available cDNAs and ESTs primarily support the three exon model, which is shown in Figure 2B. RT–PCR experiments showed that the mRNA for *AtTRM9*, were expressed in all tissues examined (stamen, rosette leaves, flowers and silique) (data not shown).

Genomic characterization of mutant plants with T-DNA insertions in the genes-encoding AtALKBH8 and AtTRM9

To investigate the role of the AtALKBH8 and AtTRM9 proteins in tRNA modification *in planta*, T-DNA insertion lines were obtained for AtALKBH8 (*atalkbh8-1*, SALK_083838C; *atalkbh8-2*, SALK_094502C) and AtTRM9 (*attrm9*, SALK_135308). The T-DNA in the *atalkbh8* lines is inserted into the gene in such a way that it disrupts the AlkB domain, while the T-DNA in the *attrm9* line is inserted shortly downstream of the translational start site in the *AtTRM9* gene (Figures 1 and 2B).

The annotated T-DNA insertions were further verified by sequencing of PCR products spanning the individual integration sites. At the LB junction in SALK_083838C (*atalkbh8-1*), the insertion point was determined to be after position 2757 in the genomic sequence of the *At1g31600* gene, corresponding to position 1634 in the mRNA sequence (NM_102896) (Figure 2D). A filler of 1 bp had been inserted between the genomic DNA and the T-DNA at this border. At the RB integration site in *atalkbh8-1,* the insertion point was determined to be at genomic position 2755 in the *At1g31600* gene, corresponding to position 1632 in the mRNA sequence (NM_102896). At this junction, a filler consisting of 20 bp scrambled genomic DNA had been integrated. Also, part of the RB sequence of the T-DNA had been deleted. In SALK_094502C (*atalkbh8-2*), there are two LB sequences integrated (Figure 2D). The integration was verified to be at position 2700 in the genomic sequence of the *At1g31600* gene, corresponding to position 1577 in the mRNA sequence (NM_102896). A filler of 30 bp was inserted between the genomic DNA and the T-DNA at this junction. The other LB junction was determined to be at genomic position 2764, corresponding to position 1642 in the mRNA sequence, showing a deletion of 64 bp at the integration site. A filler of 25 bp had been integrated at this site. Also in the SALK_135308 (*attrm9*) line, two LB sequences have been integrated (Figure 2D). The integration site of the upstream LB was determined to be at position 243 in the genomic sequence of the *At1g36310* gene, corresponding to position 161 in the mRNA sequence (NM_103320). The

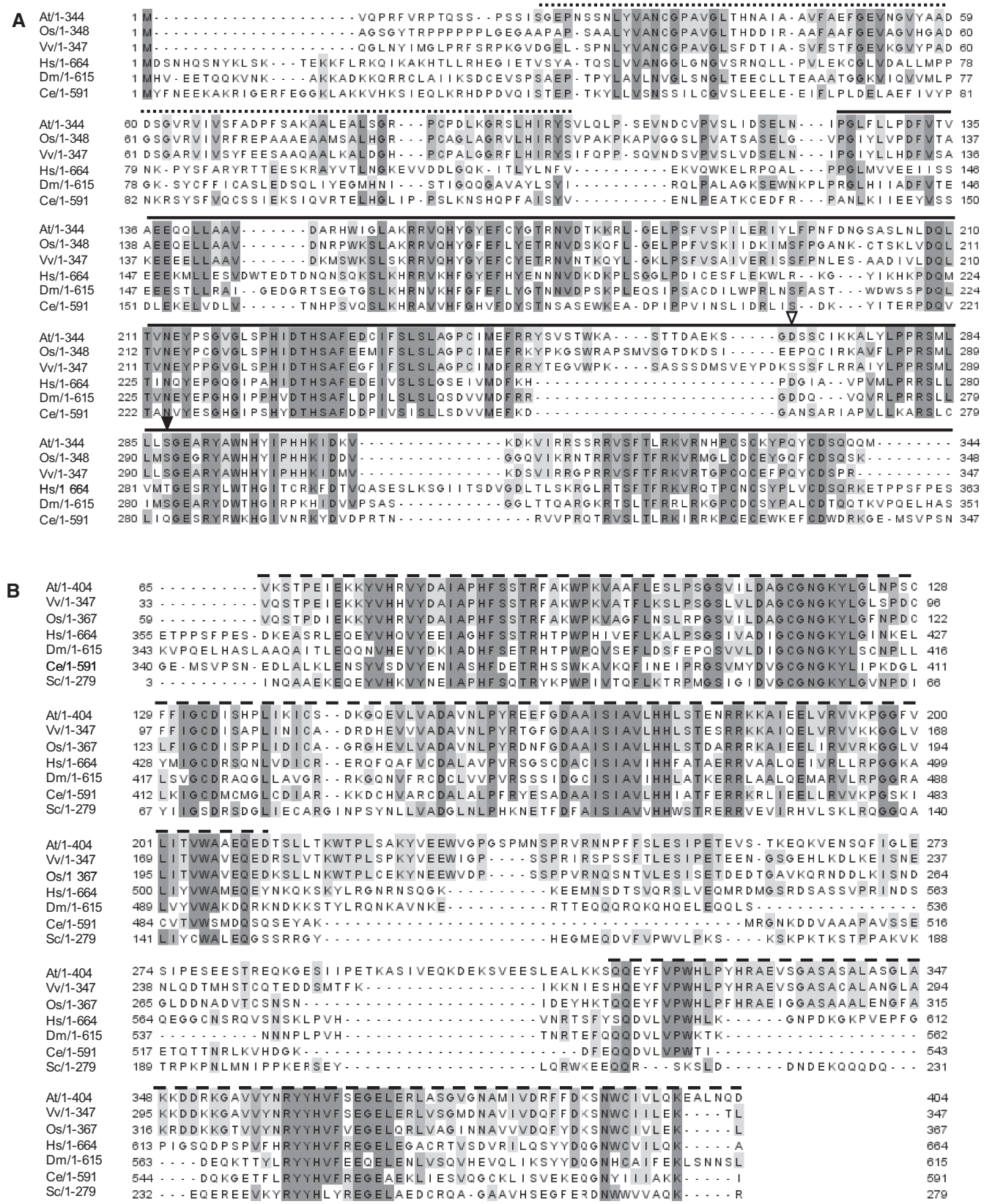

Figure 1. Protein sequence alignment of AtALKB8 and AtTRM9 with putative orthologues from selected organisms. Functional domains are indicated by dotted (RRM motif), solid (AlkB-like) and dashed (Trm9-like) lines above the alignment. (**A**) Alignment of AtALKBH8 and putative orthologues. The upstream T-DNA insertion sites in the *atalkbh8-1* and *atalkbh8-2* lines are indicated by closed and open triangles, respectively. Gene identifier numbers: Hs, *Homo sapiens*, gi|195927059; Dm, *Drosophila melanogaster*, gi|24658267; At, *Arabidopsis thaliana*, gi|42571711; Vv, *Vitis vinifera*, gi|225427651; Os, *Oryza sativa*, gi|50928501 and Ce, *Caenorhabditis elegans*, gi|17552176. (**B**) Alignment of AtTRM9 and putative

(continued)

downstream LB junction was determined to be at position 264 in the genomic sequence, corresponding to position 183 in the mRNA sequence, giving a deletion of 20 bp genomic DNA. In addition, a filler sequence of 27 bp of unknown origin was integrated at the junction.

We performed RT–PCR experiments in order to determine the expression level in the homozygous mutant lines. For the *atalkbh8-1* and *atalkbh8-2* alleles, primer pairs annealing upstream as well as downstream of the T-DNA integration site were utilized. Expression could be detected on both sides of the T-DNA insert, although considerably weaker expression was observed downstream as compared to upstream of the integration site (Figure 2E, left panel). Such downstream expression due to cryptic promoters inside the T-DNA has been shown for several other T-DNA insertion lines (30,31). However, since the T-DNA insertions in the *atalkbh8-1* and *atalkbh8-2* lines both disrupt the conserved AlkB domain of AtALKBH8, we consider it highly unlikely that a functional protein will be generated. In the *attrm9* mutant, expression downstream of the T-DNA integration site was virtually absent (Figure 2E, right panel). Full-length mRNA spanning the insertion site could not be detected in any of the mutants.

Wobble uridine modification pattern of *attrm9* and *atalkbh8* plants

The characterization of the T-DNA insertion lines shown above clearly indicated that these lines represented knockout plants with respect to the AtTRM9 or AtALKBH8 functions. However, when grown in soil, none of the homozygous mutant lines displayed any obvious morphological or developmental phenotype when compared to WT. Furthermore, the germination efficiency of seeds from these plants, as measured by scoring of testa rupture, as well as root growth were similar to that of WT plants (data not shown).

In order to investigate the potential role of these proteins in the modification of wobble uridines, we measured the levels of various modified uridines (Table 1) in total tRNA from WT and mutant plants. Total tRNA from *Arabidopsis* seedlings was digested into nucleosides and subsequently analysed by LC–MS/MS. The modifications ncm^5U, mcm^5s^2U and (*S*)-$mchm^5U$ were abundant in total tRNA from WT *Arabidopsis*, and small amounts of cm^5U, and mcm^5U were also detected (Figure 3). In addition, small amounts of ncm^5s^2U appeared to be present, but we were not able to firmly establish the presence of this modification, due to an interfering peak with similar LC retention time, and identical MS fragmentation pattern (data not shown). In contrast to the modification pattern observed in WT plants, mcm^5s^2U, (*S*)-$mchm^5U$ and mcm^5U were all virtually absent in tRNA from *attrm9* mutant plants, while the level of cm^5U, the unmethylated precursor of mcm^5U, was strongly increased (Figure 3). The levels of ncm^5U were similar in *attrm9* and WT plants, which is different from results obtained in mice and yeast, where inactivation of the Trm9 (ALKBH8-MT) function lead to an increase in the levels of this modification, as well as of the 2-thiolated derivative ncm^5s^2U (4,20). These results strongly indicate that AtTRM9 is a functional Trm9 homologue, which is required for the generation of mcm^5U in plants.

tRNA isolated from AtALKBH8-deficient plants completely lacked (*S*)-$mchm^5U$, but showed a strong increase in the levels of its precursor, mcm^5U (Figure 3), supporting the notion that AtALKBH8, like the mammalian orthologue, catalyses the hydroxylation of mcm^5U into (*S*)-$mchm^5U$. Both *atalkbh8-1* and *atalkbh8-2* mutant plants showed a virtually identical pattern of aberrant modification. Interestingly, mcm^5Um, the 2′-*O*-ribose methylated form of mcm^5U, which is present at very low levels in WT plants, was dramatically increased (~20-fold) in *atalkbh8* tRNA, indicating that a substantial portion of the accumulated mcm^5U is subjected to ribose methylation (Figure 3).

Modification status of $tRNA^{Gly}_{UCC}$ in *attrm9* and *atalkbh8* plants

(*S*)-$mchm^5U$ has been detected in a variety of ALKBH8-containing eukaryotes, including *Arabidopsis*, and it has been demonstrated that $tRNA^{Gly}_{UCC}$ from mouse, calf and silkworm contains this modification in the wobble position (12,32). The primary sequence of *Arabidopsis* $tRNA^{Gly}_{UCC}$ (retrieved from the Genomic tRNA database; http://lowelab.ucsc.edu/GtRNAdb/) is highly similar to that of silkworm and mammals, and the anticodon loop is identical (Figure 4A), suggesting that also this tRNA may carry an (*S*)-$mchm^5U$ modification. To investigate whether this is the case, an immobilized oligonucleotide of complementary sequence to $tRNA^{Gly}_{UCC}$ was used to specifically isolate this isoacceptor from total tRNA. Nucleoside analysis by LC–MS/MS clearly demonstrated a strong enrichment of (*S*)-$mchm^5U$ and the corresponding demethylated derivative, 5-[carboxy(hydroxy)methyl]uridine (chm^5U), in the isolated $tRNA^{Gly}_{UCC}$ isoacceptor, relative to total tRNA (Figure 4B and C). Note that the LC–MS/MS method used was not able to distiguish between the *R* and *S* diastereomers of chm^5U. The observed chm^5U is probably the result of spontaneous hydrolysis of the ester bond in (*S*)-$mchm^5U$, as previously reported (12). These results strongly indicated that the (*S*)-$mchm^5U$ modification is present in $tRNA^{Gly}_{UCC}$ also in *Arabidopsis*.

To study the roles of AtALKBH8 and AtTRM9 in wobble uridine modification specifically in $tRNA^{Gly}_{UCC}$, this isoacceptor was isolated from *attrm9* and *atalkbh8-1* plants. The purified isoacceptor was then digested with

Figure 1. Continued
orthologues. The upstream T-DNA insertion site in the *attrm9* line corresponds to Arg9 in the protein sequence (which is located in the non-conserved N-terminal part of the protein not included in the alignment). Gene identifier numbers: At, gi|18400083; Vv, gi|225459401; Os, gi|115448705; Hs, gi|195927059; Dm, gi|24658267; Ce, *Caenorhabditis elegans*, gi|17552176 and Sc, *Saccharomyces cerevisiae*, gi|6323627 (note that the gi numbers for AtALKBH8 and AtTRM9 homologues are identical in animals, where these two functions are carried out by a single protein).

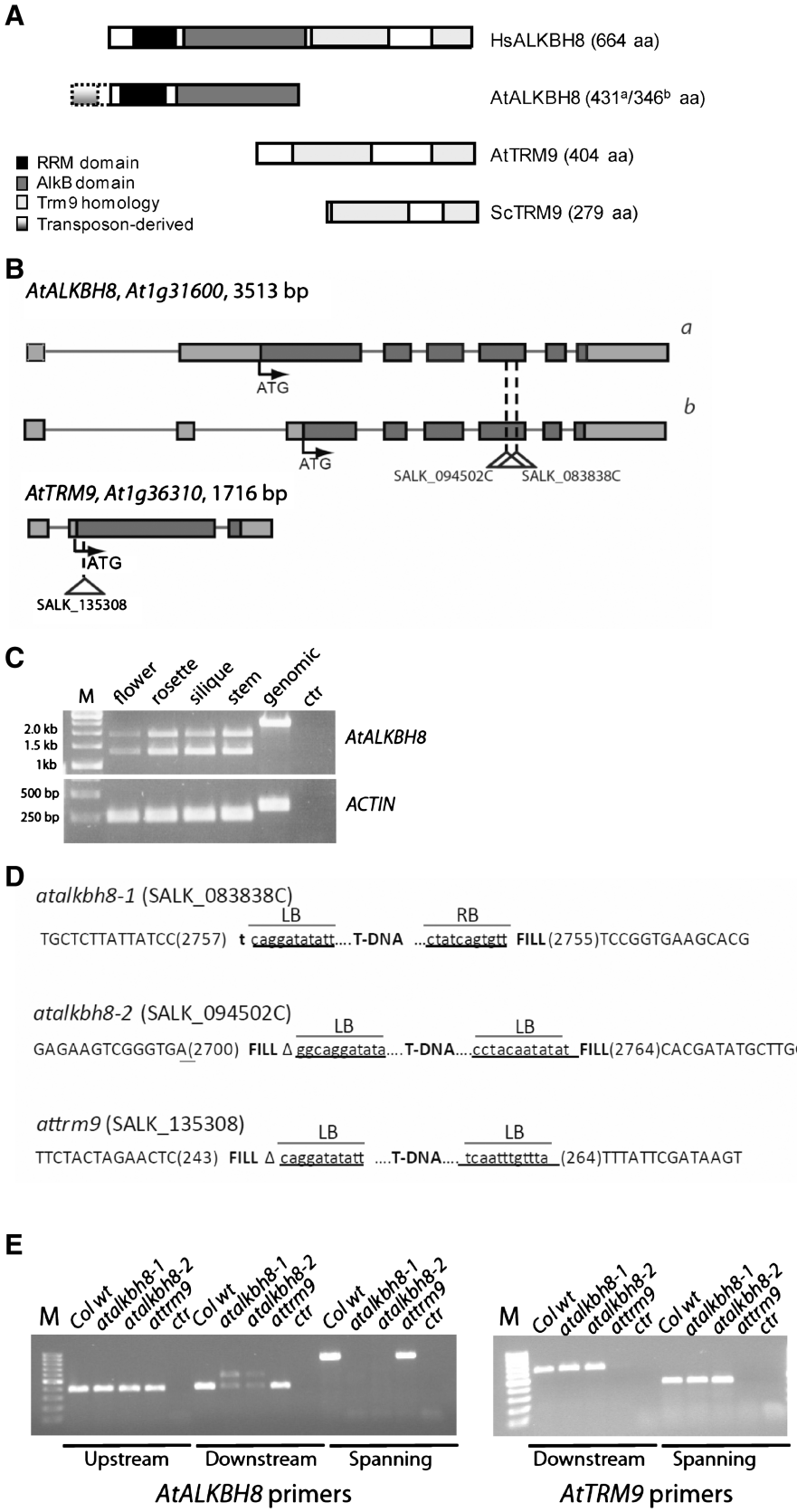

Figure 2. Architecture of the AtALKBH8 and AtTRM9 genes and characterization of corresponding T-DNA insertion lines. (**A**) Schematic view of the domain architecture of ALKBH8 and TRM9 proteins from various organisms. The N-terminal extension present in the 431 amino acid splice variant of AtALKBH8 is indicated by a dotted box, and gradient shading indicates the part of this extension, which shows strong homology to the Tag2 transposon. The RNA recognition motif is shown in black, the AlkB oxygenase in dark grey, and the methyltransferase domain is shown in

(continued)

RNase T1, which specifically cleaves 3′ to G residues, and the resulting fragments were analysed by matrix assisted laser desorption/ionization-time-of-flight (MALDI-TOF) mass spectrometry. Based on genomic tRNA sequence, the anticodon triplet of $tRNA^{Gly}_{UCC}$ is expected to be present in a 9-mer fragment of sequence CCUUCCAAG (the putatively modified wobble uridine is underlined). Indeed, fragments corresponding to mchm^{5}U and chm^{5}U modifications were detected in $tRNA^{Gly}_{UCC}$ from WT plants (Figure 4D, upper panel); a modification pattern very similar to that observed for mammalian $tRNA^{Gly}_{UCC}$ (12). It should be noted that, due to isotope distributions, each fragment gives rise to a cluster of peaks of ~1 Da spacing, where the leftmost peak corresponds to the monoisotopic mass.

When $tRNA^{Gly}_{UCC}$ from *atalkbh8-1* plants was analysed, the peak cluster corresponding to mchm^{5}U was absent, but instead a cluster corresponding to mcm^{5}U was observed (Figure 4D, middle panel), indicating that the (*S*)-mchm^{5}U modification on $tRNA^{Gly}_{UCC}$ is generated by AtALKBH8-mediated hydroxylation of mcm^{5}U. $tRNA^{Gly}_{UCC}$ derived from a*ttrm9* plants gave rise to a peak cluster that was shifted 31 Da relative to the mchm^{5}U-containing cluster. Here, the first (leftmost) peak corresponds to the monoisotopic mass of ncm^{5}U, whereas the second peak corresponds to the monoisotopic mass of cm^{5}U (Figure 4D, lower panel). Since the first peak is substantially smaller than the second one, and thereby deviates from the expected isotope pattern of a single oligonucleotide, it is highly likely that the peak cluster represents both ncm^{5}U and cm^{5}U. This is also supported by our analysis of total tRNA from *attrm9* plants, which showed an accumulation of cm^{5}U (Figure 3), as well as by our previous study from mice lacking ALKBH8-MT (the functional equivalent of Trm9), which revealed the presence of both cm^{5}U and ncm^{5}U in $tRNA^{Gly}_{UCC}$ (12). The already high levels of ncm^{5}U in total tRNA, due to the natural occurrence of this modification in many different tRNA isoacceptors, may explain why the partial modification of *attrm9* $tRNA^{Gly}_{UCC}$ by ncm^{5}U was not manifested as a significant increase in the ncm^{5}U level in total *attrm9* tRNA (Figure 3). Taken together, the data presented above show that $tRNA^{Gly}_{UCC}$ in *Arabidopsis* harbors an (*S*)-mchm^{5}U modification in the wobble position, which depends on both AtALKBH8 and AtTRM9 for its biogenesis.

The activity of AtTRM9 depends on co-expressed AtTRM112a or AtTRM112b

In mammals, the MT domain of ALKBH8 requires a small accessory protein, TRM112, to form a functional enzymatic complex (20), and it has also been shown that a similar complex is formed between yeast Trm112 and Trm9 (33). Recently, the gene *At1g22270* was shown to encode a functional *Arabidopsis* homologue of TRM112, denoted SMALL ORGAN 2 (SMO2), since *smo2* mutants show retarded organ growth due to inhibition of G_2-M phase progression during organogenesis (34). In addition to SMO2, *Arabidopsis* has another similar protein, SMO2L *(small organ 2-like)*, encoded by the gene *At1g78190*, and this protein has 78% sequence identity to SMO2. To better indicate their similarity to yeast Trm112, and to comply with the nomenclature from the NCBI protein database, we have chosen to denote these proteins AtTRM112a (SMO2) and AtTRM112b (SMO2L). Since both Trm9 and Trm112 are conserved between mammals, yeast and plants, we considered it likely that AtTRM9 may, similarly, form a functional complex with AtTRM112a or AtTRM112b. To test this, 6xHis-tagged AtTRM9 (6xHis-AtTRM9) was co-expressed in *E. coli* together with untagged AtTRM112a or AtTRM112b, and then affinity purified on TALON beads, to which 6xHis tagged proteins bind strongly. As shown in Figure 5A, a band of ~14 kDa, corresponding in size to AtTRM112a or AtTRM112b, was present on the gel after co-expression of AtTRM112a or AtTRM112b with 6xHis-AtTRM9, but not after expression of either protein alone. These results suggested that untagged AtTRM112a/b co-purified with 6xHis-AtTRM9, and that these proteins form an enzymatic complex.

The altered wobble uridine modification pattern in the AtTRM9-deficient plants indicated that this enzyme may have a function equivalent to that of yeast Trm9 and the MT moiety of mammalian ALKBH8. To investigate the putative enzymatic activity of AtTRM9 and to address the functional significance of the suggested interaction between AtTRM9 and AtTRM112a/b, purified 6xHis-AtTRM9, in the absence or presence of co-expressed AtTRM112a/AtTRM112b, was assayed for tRNA methyltransferase activity. We have previously observed that yeast tRNA, which is easily obtained in large quantities, is a good substrate for the MT activity of

Figure 2. Continued
light grey. (**B**) Schematic view of *AtALKBH8 and AtTRM9*. Exons are indicated by boxes, where putatively untranslated regions are shown in light grey and translated regions are shown in dark grey. Annotated start codons (ATG) are indicated by arrows. The upstream T-DNA insertion sites are indicated by triangles. The two alternative gene models for the AtALKBH8 locus, which give rise to the two different forms of the AtALKBH8 protein, are indicated. (**C**) Expression of mRNA encoding the two forms of AtALKBH8 in various tissues. RT–PCR on mRNA from different tissues was performed, using primers amplifying fragments of 1882 and 1302 bp representing gene model *AtALKBH8a* and *AtALKBH8b*, respectively. Genomic DNA was used as positive control (note that the genomic fragment is larger due to intron sequences). The *ACTIN2-7* gene, giving a fragment of 255 bp with primers spanning intron 2, amplified at comparable levels from all tissues, with no genomic contamination as indicated by the band of 340 bp fragment representing genomic DNA that is only seen in the genomic DNA control lane. M: Molecular weight marker. (**D**) Sequence determination of the insertion sites in the T-DNA lines. Precise location of the T-DNA in the *AtALKBH8* and *AtTRM9* genes are shown for the different lines. Exon sequences are shown in uppercase letters and left and right border (LB and RB) T-DNA sequences are underlined. Filler sequences are indicated as 'fill', while deletion of genomic DNA is marked by Δ. Numbers indicate the position of the insertion sites in the gene sequence. (**E**) Expression analysis of WT and mutant T-DNA lines by RT–PCR. Regions of the respective *AtALKBH8* (left panel) and *AtTRM9* (right panel) genes, together with relevant primer pairs (upstream, downstream or spanning the T-DNA integration site) are indicated below. For each primer set, expression analysis was conducted on mRNA from WT and different T-DNA lines as indicate above. Ctr refers to a negative control PCR sample run without cDNA, and M indicates marker lane.

Table 1. Overview of uridine modifications studied in the present work

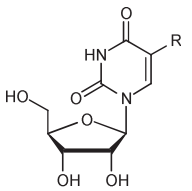

Modified uridine

R	Additional modification	Name	Abbreviation
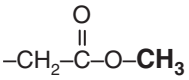	None	5-methoxycarbonyl-methyluridine	mcm^5U
	2-thio	5-methoxycarbonyl-2-thiouridine	mcm^5s^2U
	2'-O-methylribose	5-methoxycarbonyl-2′-O-methyluridine	mcm^5Um
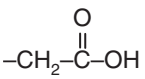	None	5-carboxymethyluridine	cm^5U
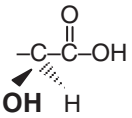	None	5-*(S)*-[carboxy(hydroxy)-methyl]uridine	(*S*)-chm^5U
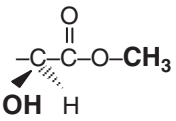	None	5-*(S)*-[methoxycarbonyl-(hydroxy)methyl]uridine	(*S*)-$mchm^5U$
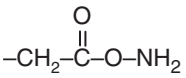	None	5-carbamoylmethyluridine	ncm^5U
	2-thio	5-carbamoylmethyl-2-thiouridine	ncm^5s^2U

The $–CH_3$ and –OH groups introduced by AtTRM9 and AtTRM8, respectively, are indicated in bold.

human ALKBH8 (20), and we therefore, considered it likely that this also may be the case for AtTRM9. To generate a substrate for the putative AtTrm9 MT activity, the yeast tRNA was subjected to mild alkaline hydrolysis referred to as saponification. This treatment causes hydrolysis of the methyl ester bond in mcm^5U and mcm^5s^2U, resulting in their conversion to the putative AtTRM9 substrates cm^5U and 5-carboxymethyl-2-thiouridine (cm^5s^2U), respectively. When saponified yeast tRNA was incubated with the radiolabelled methyl donor *S*-adenosyl-*l*-[*methyl*-^{3}H]methionine and with 6xHis-AtTRM9 that had been co-expressed with AtTRM112a or AtTRM112b, incorporation of radioactivity into tRNA was observed, supporting the notion that AtTRM9 is a functional Trm9 homolog (Figure 5B). Importantly, no incorporation of radioactivity was observed when AtTRM9 had been expressed and purified in the absence of either AtTRM112a or AtTRM112b, suggesting that interaction with AtTRM112a or AtTRM112b is required for AtTRM9 to exert its MT activity (Figure 5B).

The accumulation of cm^5U in tRNA from the *attrm9* mutant plants suggested that this tRNA may function as a MT-substrate even without saponification. Indeed, non-saponified tRNA from *attrm9* plants gave a substantially higher level of AtTRM9/AtTRM112a-mediated methylation, compared to tRNA from WT plants (Figure 5C), further supporting the notion that AtTRM9 catalyses the methylation of cm^5U into mcm^5U.

Human ALKBH8-Ox hydroxylates mcm^5U to *(S)*-$mchm^5U$ in tRNA obtained from AtALKBH8 knock-out plants

To investigate the enzymatic activity of AtALKBH8 *in vitro*, we attempted to express and purify the recombinant protein from *E. coli*, but we were unable to recover soluble protein. Instead, we addressed whether the mcm^5U-modified tRNA found in the *atalkbh8* mutant plant can function as a substrate for the ALKBH8 oxygenase activity, by treating this tRNA with the dioxygenase domain (amino acids 1–354) of human ALKBH8

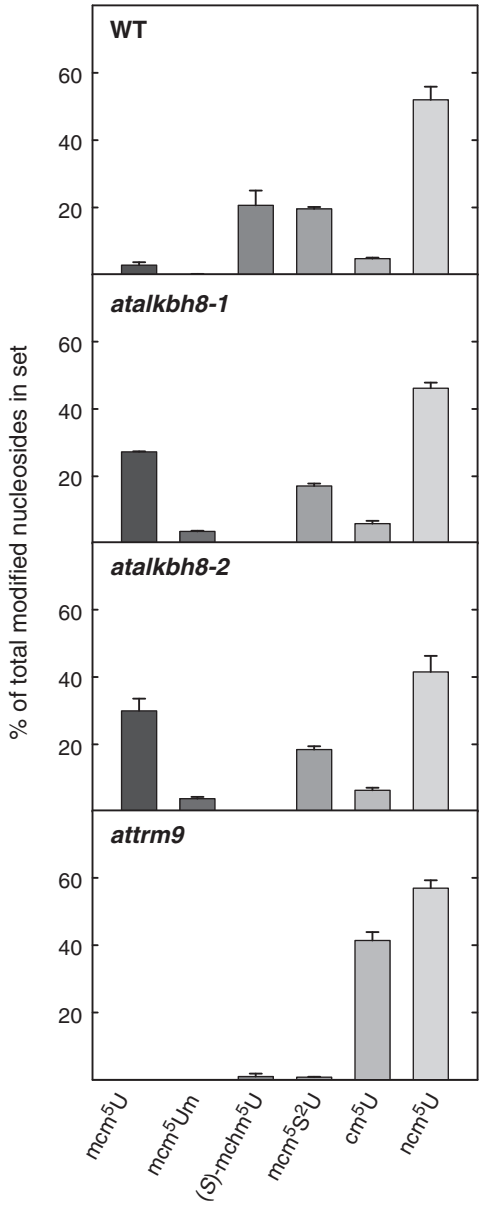

Figure 3. Wobble uridine modification status in WT, *atalkbh8* and *attrm9* plants. Total tRNA isolated from WT or mutant plants was degraded to nucleosides, and the levels of the indicated modified nucleosides were determined by LC–MS/MS analysis. The relative level of each individual modification is expressed relative to the total amount of all the shown modifications. Error bars indicate the standard deviation between triplicate samples.

(ALKBH8-Ox) and subsequently analyzed the modification status by LC–MS/MS. With increasing concentrations of enzyme, we observed an increase of (*S*)-mchm^{5}U levels accompanied by a simultaneous decrease in mcm^{5}U (Figure 5D). However, a fraction of the mcm^{5}U-modified tRNA appeared refractory to HsALKBH8-Ox-mediated hydroxylation, probably reflecting mcm^{5}U-containing isoacceptors that are not subject to further hydroxylation. These data further support that mcm^{5}U is the precursor of (*S*)-mchm^{5}U also in plants, and that AtALKBH8 is the enzyme catalyzing the hydroxylation of mcm^{5}U to (*S*)-mchm^{5}U.

DISCUSSION

Wobble uridine modifications in eukaryotic cytoplasmic tRNAs have so far mainly been studied in yeast and mammals, where a number of such modifications have been identified, along with several enzymes involved in their biogenesis. In this study, we have investigated the wobble uridine modification pattern in WT *Arabidopsis* plants and in mutants defective in enzymes putatively involved in formation of modified wobble uridines. These experiments have been complemented by enzymatic assays with recombinant enzymes, and our results establish a role for four yet uncharacterized *Arabidopsis* proteins, AtALKBH8, AtTRM9, AtTRM112a and AtTRM112b in the formation of modified wobble uridines in tRNA.

In mammals, mcm^{5}U and its 2′-*O*-ribose methylated derivative, mcm^{5}Um, are found in the wobble position of the selenocysteine specific tRNA (tRNA$^{Sec}_{UCA}$), which is responsible for the incorporation of selenocysteine into selenoproteins. The abundance of the mcm^{5}Um-modified isoform of tRNA$^{Sec}_{UCA}$, relative to its mcm^{5}U-modified counterpart, has been shown to increase in response to elevated selenium levels, and a concomitant increase in the expression of certain stress-linked selenoproteins was observed (35,36). These findings, together with studies of mice that lack the mcm^{5}Um modification, suggest that mcm^{5}Um promotes the expression of a subset of the selenoproteome and that the levels of this isoacceptor may be subject to active regulation (37,38). Thus, ribose methylation of mcm^{5}U in tRNA$^{Sec}_{UCA}$ has been proposed to be a highly specialized event, and the selenocysteine incorporation factor SECp43 was launched as a candidate specialized methyltransferase, but this has not been confirmed experimentally (39). In WT *Arabidopsis*, we detected small amounts of the mcm^{5}U modification, but the levels were elevated ~10-fold in *atalkbh8* plants. Moreover, in the *atalkbh8* mutant, we also observed substantial amounts of of mcm^{5}Um, which was virtually absent from WT plants, probably due to ribose methylation of accumulated mcm^{5}U by a non-specialized enzyme not normally dedicated to this purpose. An obvious candidate enzyme is the *Arabidopsis* homologue of *S. cerevisiae* Trm7p, which is responsible for ribose methylation of several different tRNAs in Positions 32 and/or 34 (40). Based on these results, the possibility should be considered that the mcm^{5}Um found in tRNA$^{Sec}_{UCA}$ also is a result of ribose methylation by a non-specialized enzyme, e.g. a Trm7p-homologue, and that the biological significance of this ribose methylation could be smaller than previously thought.

When the yeast Trm9 function is inactivated, tRNAs that normally contain mcm^{5}U or mcm^{5}s^{2}U instead carry a ncm^{5}U modification. When the corresponding ALKBH8 methyltransferase function is inactivated in mammals, a similar accumulation of ncm^{5}U/ncm^{5}s^{2}U was observed, as well as an accumulation of the mcm^{5}U precursor

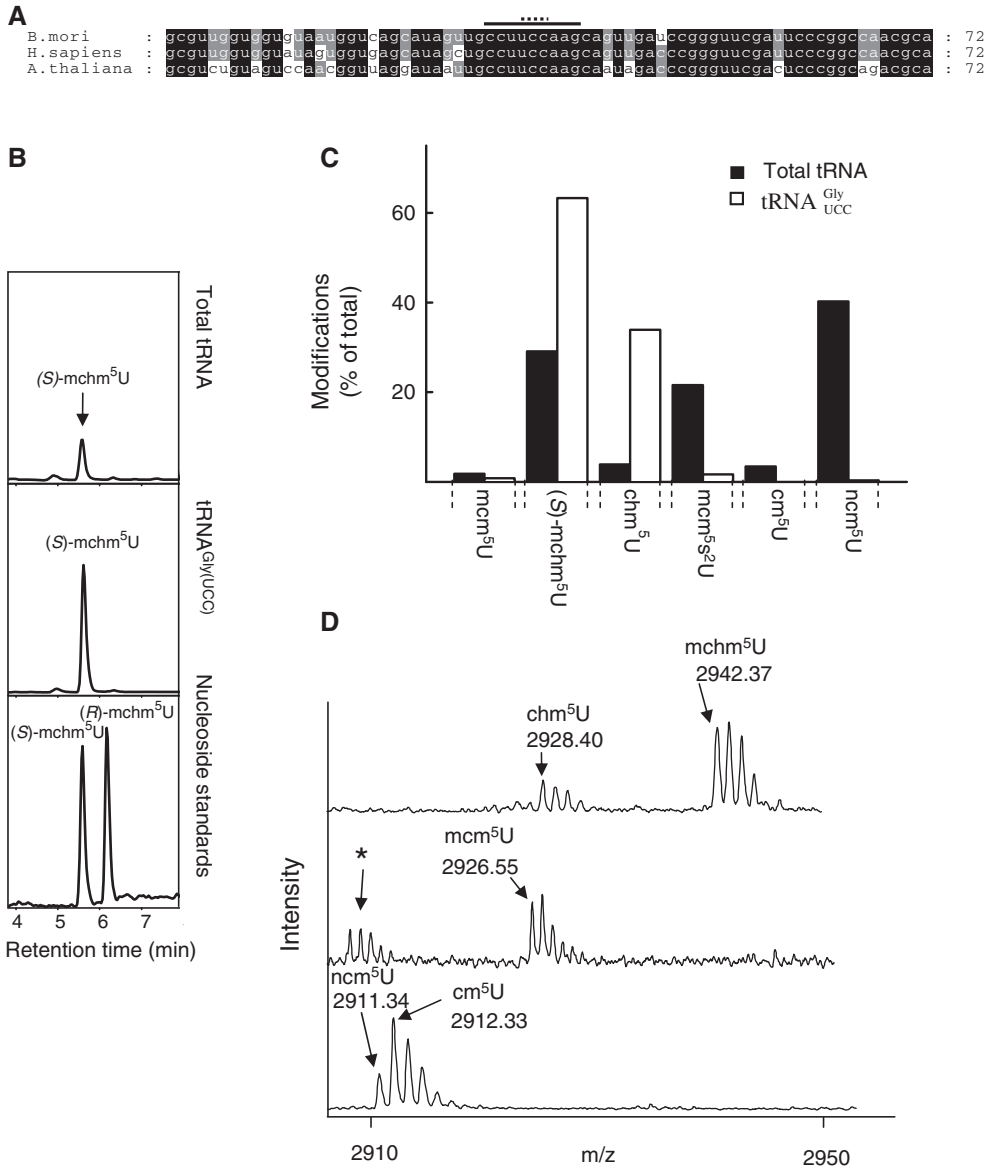

Figure 4. Wobble uridine modifications on $tRNA^{Gly}_{UCC}$ in WT, *atalkbh8* and *attrm9* plants. (**A**) Alignment of $tRNA^{Gly}_{UCC}$ from selected organisms. A solid line indicates the sequence corresponding to the anticodon loop, while the anticodon is indicated by a dotted line. (**B**) Enrichment of (*S*)-mchm^{5}U in $tRNA^{Gly}_{UCC}$ relative to WT total tRNA. LC–MS/MS analysis of (*S*)-mchm^{5}U in *Arabidopsis* $tRNA^{Gly}_{UCC}$ and in total tRNA. (**C**) Comparison of modification patterns in isolated $tRNA^{Gly}_{UCC}$ with that in total tRNA. Nucleosides were quantitated by LC–MS/MS analysis. (**D**) MALDI-TOF mass spectrometry of the anticodon fragment of $tRNA^{Gly}_{UCC}$ from WT, *atalkbh8* and *attrm9* plants. Digestion of $tRNA^{Gly}_{UCC}$ with RNase T1, which cleaves 3′ to G residues generated the anticodon fragment (indicated by a solid line in A) of primary sequence CCUUCCAAG (the wobble nucleotide is indicated). Peaks corresponding to mchm^{5}U, chm^{5}U, mcm^{5}U cm^{5}U and ncm^{5}U in the wobble position, as well as the measured masses, are indicated. An asterisk indicates minor signals from the 2′-3′-cyclic phosphate version of the fragment (the 3′-phosphate version represents the major signal). Theoretical monoisotopic mass of an anticodon fragment containing the various modifications: chm^{5}U, 2928.38; (*S*)-mchm^{5}U, 2942.40; mcm^{5}U, 2926.40; ncm^{5}U, 2911.40; cm^{5}U, 2912.39.

cm^{5}U. In the *attrm9* plants, the tRNAs that normally contain mcm^{5}U or its derivatives primarily seem to accumulate cm^{5}U, although some ncm^{5}U also appeared to be present in $tRNA^{Gly}_{UCC}$. Thus, the accumulation of cm^{5}U and/or ncm^{5}U in tRNAs that normally carry a mcm^{5}U modification seems be a general consequence of Trm9 inactivation, but the relative amounts of the accumulated cm^{5}U versus ncm^{5}U appear to vary considerably between different organisms.

Upon inactivation of the *AtALKBH8* and *AtTRM9* genes, we could see an alteration in the modification pattern that corresponded well with previous observations in transgenic mice, where only the oxygenase-function [KI(Ox^+)] or the MT-function [KI(MT^+)] of murine ALKBH8 was expressed (12). Total tRNA from the KI(Ox^+) mice showed a similar modification pattern as tRNA from *attrm9* mutant plants, as it completely lacks the mcm^{5}U modification while the levels of cm^{5}U

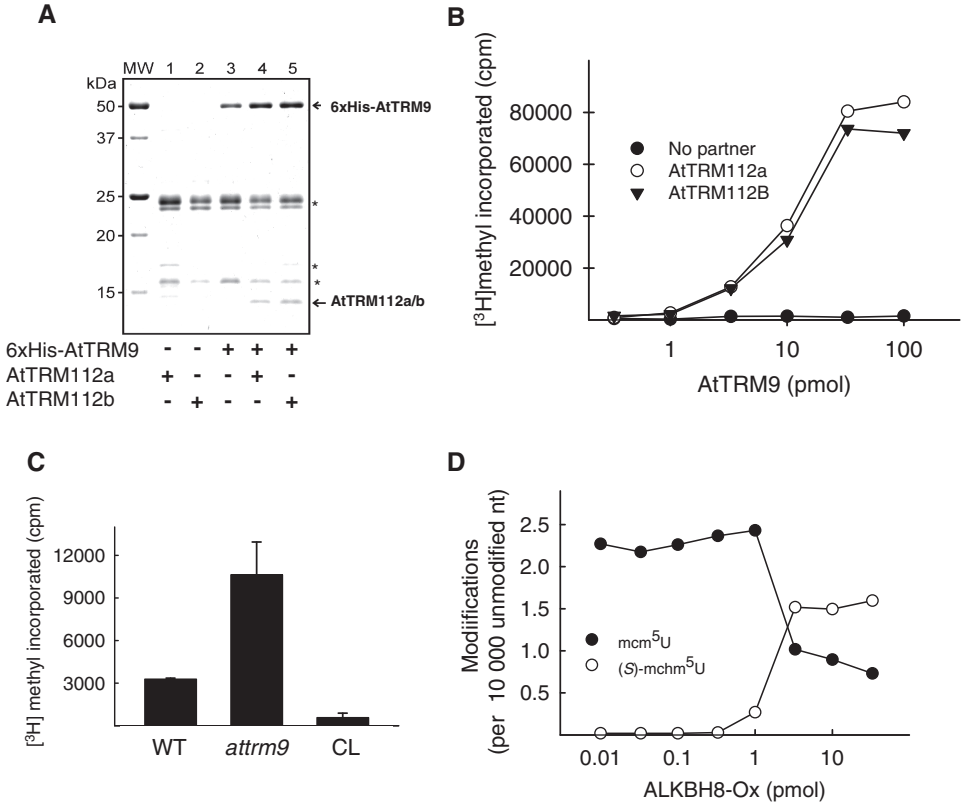

Figure 5. Activity of recombinant enzymes on WT and mutant tRNA. (**A**) Co-expression of untagged AtTRM112a and AtTRM112b with 6xHis-AtTRM9. Recombinant proteins were expressed in *E. coli*, purified by affinity chromatography on TALON beads, and then analysed by SDS–PAGE. Protein bands corresponding to AtTRM112a or AtTRM112b and AtTRM9 are indicated by arrows. Non-specific bands representing endogenous *E. coli* proteins are indicated by asterisks. (**B**) Dependence of the MT activity of AtTRM9 on co-expressed AtTRM112a or AtTRM112b. The activity was assayed on 10 µg saponified yeast tRNA using different amounts of recombinant enzyme. (**C**) AtTRM9 methyltransferase activity on tRNA from *attrm9* plants. 20 pmol AtTRM9/AtTRM112a complex was incubated with 5 µg of total tRNA from *attrm9* or WT plants, or from calf liver (CL). (**D**) Cross-species activity of human ALKBH8-Ox on *atalkbh8* tRNA. Different amounts of human ALKBH8-Ox was incubated with total tRNA from *atalkbh8* plants. The tRNA was then digested to nucleosides, and the level of mcm^5U (closed circles) and (*S*)-$mchm^5U$ (open circles) was measured by LC–MS/MS analysis.

were strongly increased. The KI(MT^+) tRNA showed a modification pattern similar to the *atalkbh8* plants, where (*S*)-$mchm^5U$ was absent, and mcm^5U was strongly increased. This clearly indicates that AtTRM9 and AtALKBH8 together perform the functions that in animals are carried out by the bifunctional ALKBH8 enzyme. The existence of bifunctional tRNA modification enzymes is not unprecedented, and one may speculate that the catalytic efficiency is improved when the product of the MT reaction can be directly channeled to the oxygenase.

Yeast Trm9 and the mammalian ALKBH8 methyltransferase both depend on the small accessory protein Trm112/TRM112 for activity (20,41). Here, we show that co-expression of AtTRM112a or AtTRM112b results in a protein of the expected size co-purifying with 6xHis-AtTRM9, and we show that the *in vitro* activity of 6x-His-AtTRM9 requires the co-expression with either AtTrm112a or AtTrm112b. Furthermore, tRNA isolated from *attrm9* plants was a better substrate for AtTRM9, as compared to WT tRNA. Taken together, these results strongly indicate that AtTRM9 has a similar function as its orthologues from yeast and mammals. The *attrm112a (smo2)* mutant of *Arabidopsis* shows a severely reduced organ growth, but this phenotype could not be reversed by expression of *AtTRM112b* (*SMO2-L)* from the *AtTRM112a* promoter. This may suggest that the *in vivo* functions of TRM112a and TRM112b are different, and that the organ growth defects seen in the *smo2* mutant are not related to the AtTRM9 MT activity.

Studies from yeast have suggested a role for Trm9 in the protection against DNA damage (42). Trm9-deficient cells are sensitive towards the methylating agent MMS; a phenotype that was explained by impaired translation of the DNA damage response genes *RNR1* and *RNR3* (42). These genes are particularly rich in the Arg codon AGA, which is decoded by a tRNA that depends on Trm9 for proper modification. We could, however, not observe any significant difference in the sensitivity towards MMS between the *attrm9* mutant and the WT plant (data not shown). This may indicate that yeast Trm9 and AtTRM9 are important for expression of different subsets of genes,

and that AtTRM9, as opposed to its yeast counterpart, is not a component in the DNA damage response machinery.

Two different forms of AtALKBH8 were identified on the mRNA level, corresponding to proteins of 344 and 431 amino acids, where the longer form contains an additional N-terminal extension. Interestingly, the major part of this extension is derived from the transposon Tag2, indicating that the long form, which is not present in other plants, has arisen through a transposition event. It has been frequently observed during genome evolution that transposon insertions generate new coding sequence or provide regulatory elements for gene expression (43). The addition of the transposon-derived extension to the AtALKBH8 coding sequence may have influenced the gene function in several conceivable ways, e.g. by adding a targeting signal for a non-cytosolic localization, by expanding the substrate specificity of the protein to allow hydroxylation of additional tRNAs, or simply by improving protein expression or increasing protein stability.

The present work represents, together with the recent characterization of mammalian ALKBH8, the only functional study of an ALKBH8 dioxygenase so far. Proteins with similarity to both the RRM and AlkB-domains of ALKBH8 appear to be present in all multicellular eukaryotes, as well as in some unicellular fungi, parasites and algae. The observation that the AtALKBH8 oxygenase, as its mammalian counterpart, is responsible for the final hydroxylation reaction leading to (*S*)-mchm^{5}U formation in $tRNA^{Gly}_{UCC}$ indicates that ALKBH8 orthologues catalyse this reaction in a wide range of organisms. Interestingly, AlkB homologues from some bacteria display a high degree of sequence similarity to the dioxygenase domain of eukaryotic ALKBH8, but they lack the RRM moiety (44,45). Several of these bacteria are plant pathogens, which may suggest that they have acquired the ALKBH8-like gene from the host during infection. Since the mcm^{5}U modification appears to be absent from bacteria, these proteins probably have an enzymatic activity different from that of eukaryotic ALKBH8, and it will be a challenge to unravel their function in future studies.

SUPPLEMENTARY DATA

Supplementary Data are available at NAR Online.

ACKNOWLEDGEMENTS

We appreciate the contribution of Marius Ulleland to the initial phase of this project. We are grateful to Anders Bekkelund, Solveig H. Engebretsen, Roy Falleth, and Mari Kjos for excellent technical assistance. We thank Angela Ho for a critical reading of the manuscript. We are grateful to Grazyna Leszczynska Andrzej Malkiewicz for providing nucleoside standards for the LC-MS/MS analysis.

FUNDING

FRIBIO and FUGE programs in the Research Council of Norway. Funding for open access charge: The Research Council of Norway.

Conflict of interest statement. None declared.

REFERENCES

1. Agris,P.F. (2004) Decoding the genome: a modified view. *Nucleic Acids Res.*, **32**, 223–238.
2. Motorin,Y. and Helm,M. (2010) tRNA stabilization by modified nucleotides. *Biochemistry*, **49**, 4934–4944.
3. Björk,G.R., Wikström,P.M. and Byström,A.S. (1989) Prevention of Translational Frameshifting by the Modified Nucleoside 1-Methylguanosine. *Science*, **244**, 986–989.
4. Johansson,M.J., Esberg,A., Huang,B., Björk,G.R. and Byström,A.S. (2008) Eukaryotic wobble uridine modifications promote a functionally redundant decoding system. *Mol. Cell. Biol.*, **28**, 3301–3312.
5. Nasvall,S.J., Chen,P. and Björk,G.R. (2004) The modified wobble nucleoside uridine-5-oxyacetic acid in tRNAPro(cmo5UGG) promotes reading of all four proline codons *in vivo*. *RNA*, **10**, 1662–1673.
6. Sprinzl,M. and Vassilenko,K.S. (2005) Compilation of tRNA sequences and sequences of tRNA genes. *Nucleic Acids Res.*, **33**, D139–D140.
7. Esberg,A., Huang,B., Johansson,M.J. and Byström,A.S. (2006) Elevated levels of two tRNA species bypass the requirement for elongator complex in transcription and exocytosis. *Mol. Cell*, **24**, 139–148.
8. Huang,B., Johansson,M.J. and Byström,A.S. (2005) An early step in wobble uridine tRNA modification requires the Elongator complex. *RNA*, **11**, 424–436.
9. Kalhor,H.R. and Clarke,S. (2003) Novel methyltransferase for modified uridine residues at the wobble position of tRNA. *Mol. Cell. Biol.*, **23**, 9283–9292.
10. Björk,G.R., Huang,B., Persson,O.P. and Byström,A.S. (2007) A conserved modified wobble nucleoside (mcm5s2U) in lysyl-tRNA is required for viability in yeast. *RNA*, **13**, 1245–1255.
11. Amberg,R., Urban,C., Reuner,B., Scharff,P., Pomerantz,S.C., McCloskey,J.A. and Gross,H.J. (1993) Editing does not exist for mammalian selenocysteine tRNAs. *Nucleic Acids Res.*, **21**, 5583–5588.
12. van den Born,E., Vagbø,C.B., Songe-Møller,L., Leihne,V., Lien,G.F., Leszczynska,G., Malkiewicz,A., Krokan,H.E., Kirpekar,F., Klungland,A. *et al.* (2011) ALKBH8-mediated formation of a novel diastereomeric pair of wobble nucleosides in mammalian tRNA. *Nat. Commun.*, **2**, 172.
13. Aas,P.A., Otterlei,M., Falnes,P.Ø., Vagbø,C.B., Skorpen,F., Akbari,M., Sundheim,O., Bjoras,M., Slupphaug,G., Seeberg,E. *et al.* (2003) Human and bacterial oxidative demethylases repair alkylation damage in both RNA and DNA. *Nature*, **421**, 859–863.
14. Duncan,T., Trewick,S.C., Koivisto,P., Bates,P.A., Lindahl,T. and Sedgwick,B. (2002) Reversal of DNA alkylation damage by two human dioxygenases. *Proc. Natl Acad. Sci. USA*, **99**, 16660–16665.
15. Falnes,P.Ø., Johansen,R.F. and Seeberg,E. (2002) AlkB-mediated oxidative demethylation reverses DNA damage in *Escherichia coli*. *Nature*, **419**, 178–182.
16. Gerken,T., Girard,C.A., Tung,Y.C., Webby,C.J., Saudek,V., Hewitson,K.S., Yeo,G.S., McDonough,M.A., Cunliffe,S., McNeill,L.A. *et al.* (2007) The obesity-associated FTO gene encodes a 2-oxoglutarate-dependent nucleic acid demethylase. *Science*, **318**, 1469–1472.
17. Kurowski,M.A., Bhagwat,A.S., Papaj,G. and Bujnicki,J.M. (2003) Phylogenomic identification of five new human homologs of the DNA repair enzyme AlkB. *BMC Genomics*, **4**, 48.

18. Trewick,S.C., Henshaw,T.F., Hausinger,R.P., Lindahl,T. and Sedgwick,B. (2002) Oxidative demethylation by Escherichia coli AlkB directly reverts DNA base damage. *Nature*, **419**, 174–178.
19. Fu,D., Brophy,J.A., Chan,C.T., Atmore,K.A., Begley,U., Paules,R.S., Dedon,P.C., Begley,T.J. and Samson,L.D. (2010) Human AlkB homolog ABH8 Is a tRNA methyltransferase required for wobble uridine modification and DNA damage survival. *Mol. Cell. Biol.*, **30**, 2449–2459.
20. Songe-Møller,L., van den Born,E., Leihne,V., Vagbø,C.B., Kristoffersen,T., Krokan,H.E., Kirpekar,F., Falnes,P.Ø. and Klungland,A. (2010) Mammalian ALKBH8 possesses tRNA methyltransferase activity required for the biogenesis of multiple wobble uridine modifications implicated in translational decoding. *Mol. Cell. Biol.*, **30**, 1814–1827.
21. Fu,Y., Dai,Q., Zhang,W., Ren,J., Pan,T. and He,C. (2010) The AlkB domain of mammalian ABH8 catalyzes hydroxylation of 5-methoxycarbonylmethyluridine at the wobble position of tRNA. *Angew.Chem. Int. Ed. Engl.*, **49**, 8885–8888.
22. Golovko,A., Sitbon,F., Tillberg,E. and Nicander,B. (2002) Identification of a tRNA isopentenyltransferase gene from *Arabidopsis thaliana*. *Plant Mol. Biol.*, **49**, 161–169.
23. Goll,M.G., Kirpekar,F., Maggert,K.A., Yoder,J.A., Hsieh,C.L., Zhang,X., Golic,K.G., Jacobsen,S.E. and Bestor,T.H. (2006) Methylation of tRNAAsp by the DNA methyltransferase homolog Dnmt2. *Science*, **311**, 395–398.
24. Mehlgarten,C., Jablonowski,D., Wrackmeyer,U., Tschitschmann,S., Sondermann,D., Jager,G., Gong,Z., Byström,A.S., Schaffrath,R. and Breunig,K.D. (2010) Elongator function in tRNA wobble uridine modification is conserved between yeast and plants. *Mol. Microbiol.*, **76**, 1082–1094.
25. Chen,P., Jager,G. and Zheng,B. (2010) Transfer RNA modifications and genes for modifying enzymes in *Arabidopsis thaliana*. *BMC Plant Biol.*, **10**, 201.
26. Katoh,K., Kuma,K., Toh,H. and Miyata,T. (2005) MAFFT version 5: improvement in accuracy of multiple sequence alignment. *Nucleic Acids Res.*, **33**, 511–518.
27. Waterhouse,A.M., Procter,J.B., Martin,D.M., Clamp,M. and Barton,G.J. (2009) Jalview Version 2—a multiple sequence alignment editor and analysis workbench. *Bioinformatics*, **25**, 1189–1191.
28. Murashige,T. and Skoog,F. (1962) A Revised Medium for Rapid Growth and Bio Assays with Tobacco Tissue Cultures. *Physiologia Plantarum*, **15**, 473–497.
29. Henk,A.D., Warren,R.F. and Innes,R.W. (1999) A new Ac-like transposon of *Arabidopsis* is associated with a deletion of the RPS5 disease resistance gene. *Genetics*, **151**, 1581–1589.
30. Chen,I.P., Mannuss,A., Orel,N., Heitzeberg,F. and Puchta,H. (2008) A homolog of ScRAD5 is involved in DNA repair and homologous recombination in *Arabidopsis*. *Plant Physiol.*, **146**, 1786–1796.
31. Hartung,F., Suer,S. and Puchta,H. (2007) Two closely related RecQ helicases have antagonistic roles in homologous recombination and DNA repair in *Arabidopsis* thaliana. *Proc. Natl Acad. Sci. USA*, **104**, 18836–18841.
32. Kawakami,M., Takemura,S., Kondo,T., Fukami,T. and Goto,T. (1988) Chemical structure of a new modified nucleoside located in the anticodon of Bombyx mori glycine tRNA2. *J. Biochem.*, **104**, 108–111.
33. Purushothaman,S.K., Bujnicki,J.M., Grosjean,H. and Lapeyre,B. (2005) Trm11p and Trm112p are both required for the formation of 2-methylguanosine at position 10 in yeast tRNA. *Mol. Cell. Biol.*, **25**, 4359–4370.
34. Hu,Z., Qin,Z., Wang,M., Xu,C., Feng,G., Liu,J., Meng,Z. and Hu,Y. (2010) The Arabidopsis SMO2, a homologue of yeast TRM112, modulates progression of cell division during organ growth. *Plant J*, **61**, 600–610.
35. Diamond,A.M., Choi,I.S., Crain,P.F., Hashizume,T., Pomerantz,S.C., Cruz,R., Steer,C.J., Hill,K.E., Burk,R.F., McCloskey,J.A. *et al.* (1993) Dietary selenium affects methylation of the wobble nucleoside in the anticodon of selenocysteine tRNA([Ser]Sec). *J. Biol. Chem.*, **268**, 14215–14223.
36. Jameson,R.R. and Diamond,A.M. (2004) A regulatory role for Sec tRNA[Ser]Sec in selenoprotein synthesis. *RNA*, **10**, 1142–1152.
37. Carlson,B.A., Xu,X.M., Gladyshev,V.N. and Hatfield,D.L. (2005) Selective rescue of selenoprotein expression in mice lacking a highly specialized methyl group in selenocysteine tRNA. *J. Biol. Chem.*, **280**, 5542–5548.
38. Moustafa,M.E., Carlson,B.A., El-Saadani,M.A., Kryukov,G.V., Sun,Q.A., Harney,J.W., Hill,K.E., Combs,G.F., Feigenbaum,L., Mansur,D.B. *et al.* (2001) Selective inhibition of selenocysteine tRNA maturation and selenoprotein synthesis in transgenic mice expressing isopentenyladenosine-deficient selenocysteine tRNA. *Mol. Cell. Biol.*, **21**, 3840–3852.
39. Hatfield,D.L., Carlson,B.A., Xu,X.M., Mix,H. and Gladyshev,V.N. (2006) Selenocysteine incorporation machinery and the role of selenoproteins in development and health. *Prog. Nucleic Acid Res. Mol. Biol.*, **81**, 97–142.
40. Pintard,L., Lecointe,F., Bujnicki,J.M., Bonnerot,C., Grosjean,H. and Lapeyre,B. (2002) Trm7p catalyses the formation of two 2′-O-methylriboses in yeast tRNA anticodon loop. *EMBO J.*, **21**, 1811–1820.
41. Studte,P., Zink,S., Jablonowski,D., Bar,C., von der,H.T., Tuite,M.F. and Schaffrath,R. (2008) tRNA and protein methylase complexes mediate zymocin toxicity in yeast. *Mol. Microbiol.*, **69**, 1266–1277.
42. Begley,U., Dyavaiah,M., Patil,A., Rooney,J.P., DiRenzo,D., Young,C.M., Conklin,D.S., Zitomer,R.S. and Begley,T.J. (2007) Trm9-catalyzed tRNA modifications link translation to the DNA damage response. *Mol. Cell*, **28**, 860–870.
43. Feschotte,C. and Pritham,E.J. (2007) DNA transposons and the evolution of eukaryotic genomes. *Annu. Rev. Genet.*, **41**, 331–368.
44. Falnes,P.Ø. and Rognes,T. (2003) DNA repair by bacterial AlkB proteins. *Res. Microbiol.*, **154**, 531–538.
45. van den Born,E., Bekkelund,A., Moen,M.N., Omelchenko,M.V., Klungland,A. and Falnes,P.Ø. (2009) Bioinformatics and functional analysis define four distinct groups of AlkB DNA-dioxygenases in bacteria. *Nucleic Acids Res.*, **21**, 7124–7136.